
Mixed-Variable Bayesian Optimization

Erik Daxberger^{*,1,2,†} Anastasia Makarova^{*,3} Matteo Turchetta^{*,2,3} Andreas Krause³
¹ University of Cambridge ² MPI for Intelligent Systems ³ ETH Zurich

Abstract

The optimization of expensive to evaluate, black-box, mixed-variable functions, i.e. functions that have continuous and discrete inputs, is a difficult and yet pervasive problem in science and engineering. In Bayesian optimization (BO), special cases of this problem that consider fully continuous or fully discrete domains have been widely studied. However, few methods exist for mixed-variable domains. In this paper, we introduce MIVABO, a novel BO algorithm for the efficient optimization of mixed-variable functions that combines a linear surrogate model based on expressive feature representations with Thompson sampling. We propose two methods to optimize its acquisition function, a challenging problem for mixed-variable domains, and we show that MIVABO can handle complex constraints over the discrete part of the domain that other methods cannot take into account. Moreover, we provide the first convergence analysis of a mixed-variable BO algorithm. Finally, we show that MIVABO is significantly more sample efficient than state-of-the-art mixed-variable BO algorithms on hyperparameter tuning tasks.

1 Introduction

Bayesian optimization (BO) [37] is a well-established paradigm to optimize costly-to-evaluate, black-box objectives that has been successfully applied to multiple scientific domains. Most of the existing BO literature focuses on objectives that have purely *continuous* domains, such as those arising in tuning of continuous hyperparameters of machine learning algorithms, recommender systems, and preference learning [55]. More recently, problems with purely *discrete* domains, such as food safety control and model-sparsification in multi-component systems [4] have been considered.

However, many real-world optimization problems in applied mathematics, engineering and the natural sciences are of *mixed-variable* nature, involving *both* continuous and discrete input variables, and exhibit complex constraints. For example, tuning the hyperparameters of a convolutional neural network involves both continuous variables, e.g., learning rate and momentum, and discrete ones, e.g., kernel size, stride and padding. In addition, these hyperparameters impose validity constraints, e.g., there are combinations of kernel size, stride and padding that lead to invalid networks. Further examples of mixed-variable, potentially constrained, optimization problems include sensor placement [32], drug discovery [39], configuration of optimization solvers [24] and many others. In this work, we introduce an algorithm that can efficiently optimize mixed-variable functions subject to known constraints.

Related Work. The efficient optimization of black-box functions over continuous domains has been extensively studied in the BO literature [58, 62, 20]. However, to adapt these methods to the mixed-variable setting, it is necessary to use ad-hoc relaxation techniques to map the problem to a fully continuous one and rounding methods to map the resulting solution to the original domain. This procedure ignores the original structure of the domain and makes the quality of the solution dependent on the choice of relaxation and rounding methods. Moreover, in this setting, it is hard to

*Equal contribution. †Work done while at ETH Zurich. Correspondence to: E.D. <ead54@cam.ac.uk>.

incorporate constraints over the discrete input variables. More recently, BO algorithms for discrete domains have been proposed [4, 42]. However, the application of these methods to the mixed-variable setting requires discretizing the continuous part of the domain, where the discretization granularity plays a crucial role: If it is too small, it makes the input space prohibitively large; if it is too large, the resulting domain may contain only poorly performing values of the continuous inputs.

Few BO methods can directly solve mixed-variable optimization problems. For example, SMAC [25] uses a random forest as a surrogate model, which accommodates for mixed-variable inputs. However, the frequentist uncertainty estimate provided by random forests may suffer from variance degradation and may not be accurate enough to steer the sampling. The TPE algorithm [5] uses non-parametric kernel density estimators (KDEs) to identify inputs that are likely to improve upon and unlikely to perform worse than the best input found so far. Due to the nature of KDEs, TPE naturally supports mixed input spaces. Moreover, its inference step is computationally efficient. While SMAC and TPE can handle hierarchical constraints, they cannot handle more general constraints over the discrete variables. Moreover, they do not have any convergence guarantees. Hyperband (HB) [34] is a variant of random search that exploits cheap but less accurate approximations of the objective to dynamically allocate resources for function evaluations. BOHB [14] is the model-based counterpart of HB, based on TPE. Therefore, they extend existing mixed-variable optimization methods to the multi-fidelity setting rather than proposing new ones. As such, their core idea is complementary to our method, rather than in competition with it. Surrogate modeling over a mixed-variable domain is addressed in [3]; however, they don't consider acquisition function optimization, which is a challenging problem, especially in mixed-variable domains. Moreover, the authors leave the important part of choosing the model features to its user. The approach proposed in [15] solves mixed-variable acquisition function optimization by simply using continuous optimization oracles and rounding the result, thus it does not explicitly account for the different variable types. As a result, they are unable to show any convergence guarantees and handle linear and quadratic constraints on the discrete variables.

Contributions. We introduce MiVABO, a novel algorithm for the efficient optimization of mixed-variable functions subject to known integer linear and quadratic constraints. It is based on a linear surrogate model that decouples the continuous and discrete components of the function from the mixed one using an expressive feature expansion (Section 3.1). We exploit the ability of this model to efficiently draw samples from the posterior over the objective that can be evaluated at every point in the domain (Section 3.2), by combining it with Thompson sampling. Moreover, we present two alternatives to optimize the resulting acquisition function that can incorporate known linear and quadratic constraints (Section 3.3). To the best of our knowledge, this makes MiVABO the first BO method that can handle constraints over discrete variables. Notice that, while in continuous BO, the optimization of the acquisition function is difficult but has well established solutions, the latter is not the case for the mixed-variable case and solving this problem efficiently is a key challenge. Moreover, we provide the first convergence analysis of a mixed-variable BO algorithm (Section 3.4). Finally, we demonstrate the effectiveness of MiVABO on complex hyperparameter optimization tasks, such as deep generative model tuning, where it outperforms state-of-the-art methods and performs comparably to human expert tuning (Section 4).

2 Problem Statement

We consider the problem of optimizing an unknown and expensive-to-evaluate, scalar-valued function defined over a mixed-variable domain, accessible through noise-perturbed evaluations and subject to known linear and quadratic constraints. Formally, we aim to solve

$$\min_{\mathbf{x} \in \mathcal{X}} f(\mathbf{x}) \quad \text{s.t. } g^c(\mathbf{x}) \geq 0, \quad g^d(\mathbf{x}) \geq 0, \quad (1)$$

where $\mathcal{X} \subseteq \mathcal{X}^c \times \mathcal{X}^d$, with \mathcal{X}^c and \mathcal{X}^d being continuous and discrete subspaces and where $g^c(\mathbf{x}) \geq 0$ and $g^d(\mathbf{x}) \geq 0$ represent a set of known linear and quadratic constraints defined over the continuous and discrete parts of the domain, respectively. We assume that the continuous variables live in a box-constrained domain which, w.l.o.g., can be scaled to the unit hypercube. Therefore, we have $\mathcal{X}^c = [0, 1]^{D_c}$. Furthermore, we assume w.l.o.g. that the discrete variables are binary, i.e. that vectors $\mathbf{x}^d \in \mathcal{X}^d$ correspond to vertices of the unit hypercube. Therefore, we have $\mathcal{X}^d = \{0, 1\}^{D_d}$. Note that this binary representation can be used to describe any discrete space, and may thus serve

as the domain space of any discrete function. For example, a vector $\mathbf{x}^d = [x_1^d, \dots, x_{D_d}^d] \in \mathcal{X}^d$ could correspond to a subset A of some ground set $\mathcal{V} = \{v_1, \dots, v_{D_d}\}$ of D_d discrete elements, such that $x_i^d = 1 \Leftrightarrow a_i \in A$ and $x_i^d = 0 \Leftrightarrow a_i \notin A$, thus yielding a set function. Alternatively, a vector $\mathbf{x}^d \in \mathcal{X}^d$ could correspond to a binary encoding of one or more (non-binary) integer-valued variables, thus resulting in a function defined on an integral domain.

Background. Bayesian optimization (BO) algorithms are iterative black-box optimization methods where, at every step t , we select an input $\mathbf{x}_t \in \mathcal{X}$ and observe a noise-perturbed output $y_t \triangleq f(\mathbf{x}_t) + \epsilon$ with $\epsilon \stackrel{\text{iid}}{\sim} \mathcal{N}(0, \beta^{-1})$, where $\beta > 0$. Since evaluating f is costly, the goal is to query inputs based on past observations to find a global minimizer $\mathbf{x}_* \in \arg \min_{\mathbf{x} \in \mathcal{X}} f(\mathbf{x})$ as efficiently and accurately as possible. To this end, BO algorithms leverage two components: (i) a *probabilistic function model*, also known as surrogate, that encodes the belief about f based on the observations available, and (ii) an *acquisition function* $\alpha : \mathcal{X} \rightarrow \mathbb{R}$ that expresses the informativeness of input \mathbf{x} about the location of \mathbf{x}_* , given the surrogate of f . Based on our belief about the objective, encoded by the probabilistic model, we query the most informative input, measured by the acquisition function. We then update the model with the resulting observation and repeat this procedure. The goal of the acquisition function is to simultaneously learn about the inputs that are likely to be optimal and about poorly explored regions of the input space, i.e. to trade-off exploitation against exploration.

Thus, BO reduces the initial challenging black-box optimization problem to a series of cheaper optimization problems $\mathbf{x}_t \in \arg \max_{\mathbf{x} \in \mathcal{X}} \alpha_t(\mathbf{x})$. However, in our case, these are mixed-variable optimization problems that exhibit linear and quadratic constraints and, therefore, still challenging. In the next section, we present a surrogate model, an acquisition function and two acquisition function optimization routines that, combined, allow us to efficiently solve the problem in Eq. (1).

3 MIVABO Algorithm

We first introduce the linear model used to represent the objective (Sec. 3.1) and describe how to do inference for it. (Sec. 3.2). We then show how to use Thompson sampling [59] to suggest informative inputs to query (Sec. 3.3) and, finally, provide a bound on the regret incurred by MIVABO. (Sec. 3.4).

3.1 Model

We introduce a surrogate model of the objective that accounts for both discrete and continuous input variables in a principled way, while balancing the following, conflicting goals. On the one hand, we want a complex and expressive model that can capture or, at least, approximate a large class of real-world functions. On the other hand, excessively complex models may render Bayesian inference and constrained optimization of the mixed-variable acquisition computationally infeasible.

Linear models defined over non-linear feature mappings of the inputs, $f(\mathbf{x}) = \mathbf{w}^\top \phi(\mathbf{x})$, are a class of flexible parametric models that strike a good trade-off between model capacity, interpretability and ease of use through the definition of the non-linear features $\phi : \mathcal{X} \rightarrow \mathbb{R}^M$. For example, in this class of models, Bayesian inference scales linearly in the number of data points and cubically in the number of features, M [8]. While the complexity of the model is controlled by the number of its features, its capacity depends on their definition. Therefore, to simplify and make more intuitive the problem of designing a set of expressive features, we treat separately the contribution to the objective f coming from the continuous part of the domain, from the discrete one and from the interaction of the two,

$$f(\mathbf{x}) = \mathbf{w}^d{}^\top \phi^d(\mathbf{x}^d) + \mathbf{w}^c{}^\top \phi^c(\mathbf{x}^c) + \mathbf{w}^m{}^\top \phi^m(\mathbf{x}^d, \mathbf{x}^c), \quad (2)$$

where, for $j \in \{d, c, m\}$, $\phi^j(\mathbf{x}^j) = [\phi_i^j(\mathbf{x}^j)]_{i=1}^{M_j} \in \mathbb{R}^{M_j}$ and $\mathbf{w}^j \in \mathbb{R}^{M_j}$ denote the feature and weight vector for the discrete, continuous and mixed component, respectively. Importantly, given a sample from the posterior distribution over the weights, the corresponding function can be easily evaluated at any point in the domain, which is important for optimizing the acquisition function.²

In many real-world problems, a large portion of possible features can be discarded a priori, simplifying the design space. A common assumption in BO (especially in high-dimensional BO) is that,

²The importance of this will become clear in Section 3.3 when we describe how Thompson sampling works.

for real-world functions, only low-order interactions between the variables contribute significantly to the objective function. This was shown to be the case for many practical problems [23, 49, 38], including hyperparameter tuning of deep neural networks [19]. Based on this assumption, we focus on features defined over small subsets of the input variables. Formally, $\phi(\mathbf{x}) = [\phi_k(\mathbf{x}_k)]_{k=1}^M$, where \mathbf{x}_k is a subvector of \mathbf{x} which may exclusively contain some of the continuous variables, exclusively some of the discrete ones, or some of both types. Accordingly, the objective $f(\mathbf{x})$ can be decomposed into a sum of functions $f_k(\mathbf{x}_k) \triangleq w_k \phi_k(\mathbf{x}_k)$ defined over subvectors \mathbf{x}_k from low-dimensional subspaces $\mathcal{X}_k \subseteq \mathcal{X}$ with $\dim(\mathcal{X}_k) \ll \dim(\mathcal{X})$. Such a model decomposition is also known as a *generalized additive model* [49, 18], where it is assumed that a variable can be included in more than one subvector, i.e. $j \neq k \nRightarrow \mathcal{X}_j \cap \mathcal{X}_k = \emptyset$. The complexity of such a model can be controlled by the effective dimensionality of the subspaces. This is important in case of computational resource restrictions. In particular, let $\bar{D}_d \triangleq \max_{k \in [M]} \dim(\mathcal{X}_k^d)$ denote the effective dimensionality of the discrete component in Eq. (2), i.e. the dimensionality of the largest among all subspaces that exclusively contains discrete variables. Analogously, \bar{D}_c and \bar{D}_m denote the effective continuous and mixed dimensionalities, respectively. Intuitively, the effective dimensionality corresponds to the maximum order of the variable interactions present in f . The number of features $M = \mathcal{O}(\bar{D}_d^{\bar{D}_d} + \bar{D}_c^{\bar{D}_c} + (\bar{D}_d + \bar{D}_c)^{\bar{D}_m})$ then scales exponentially in the effective dimensionalities only³, which are usually small, even if the true dimensionality is large.

Discrete Features ϕ^d . We aim at defining a set of features, ϕ^d , that can effectively represent the discrete component of Eq. (2) as a linear function. Generally, the model should be able to capture arbitrary interactions between the discrete variables. To do so, we consider all subsets S of the discrete variables in \mathcal{X}^d (or equivalently, all elements S of the powerset $2^{\mathcal{X}^d}$ of \mathcal{X}^d) and define a monomial $\prod_{j \in S} x_j^d$ for each subset S (where for the empty set, $\prod_{j \in \emptyset} x_j^d = 1$). We then construct a weighted sum of all these monomials to arrive at the multi-linear polynomial $\mathbf{w}^{d^\top} \phi^d(\mathbf{x}^d) = \sum_{S \in 2^{\mathcal{X}^d}} w_S \prod_{j \in S} x_j^d$. This functional representation also corresponds to the Fourier expansion of a so-called *pseudo-Boolean function* (PBF) [9, 41]. In practice, an exponential number of features can be prohibitively expensive and may lead to high-variance estimators as in BO one typically does not have access to massive amounts of data to robustly fit a large model [16]. Alternatively, [4, 19] empirically found that a second-order polynomial in the Fourier basis provides a practical balance between expressiveness and efficiency, even when the true function is of higher order. In our model, we also consider quadratic PBFs, $\mathbf{w}^{d^\top} \phi^d(\mathbf{x}^d) = w_\emptyset + \sum_{i=1}^n w_{\{i\}} x_i^d + \sum_{1 \leq i < j \leq n} w_{\{i,j\}} x_i^d x_j^d$, which induces the discrete feature representation $\phi^d(\mathbf{x}^d) \triangleq [1, \{x_i^d\}_{i=1}^{\bar{D}_d}, \{x_i^d x_j^d\}_{1 \leq i < j \leq \bar{D}_d}]^\top$ and reduces the number of weights in the surrogate model to $M_d \in \mathcal{O}(\bar{D}_d^2)$.

Continuous Features ϕ^c . In BO over continuous spaces, most approaches are based on non-parametric Gaussian process (GP) models [63] due to their flexibility and ability to capture large classes of continuous functions. To fit our linear model formulation, we leverage GPs' expressiveness by modeling the continuous part of our model in Eq. (2) using feature expansions $\phi^c(\mathbf{x}^c)$ that result in a finite linear approximation of a GP. One conceptually simple yet theoretically well-founded choice of such a basis expansion, which we also use in our experiments, is the celebrated class of Random Fourier Features (RFF) [45, 46], which induce a randomized approximation of a GP based on Monte Carlo integration. Alternatively, one can leverage Quadrature Fourier Features (QFF) [38], which instead use a deterministic approximation based on numerical integration, and which are particularly effective for problems with low effective dimensionality. Both methods have been successfully applied in BO [27, 44, 38]. Alternatively, one can also use features learned from data via a neural network [56].

Mixed Features ϕ^m . The goal of the mixed term is to capture as rich and realistic interactions between the discrete and continuous variables as possible, while keeping model inference and acquisition function optimization efficient. To this end, we stack products of all pairwise combinations of features of the two variable types, i.e. $\phi^m(\mathbf{x}^d, \mathbf{x}^c) \triangleq [\phi_i^d(\mathbf{x}^d) \cdot \phi_j^c(\mathbf{x}^c)]_{1 \leq i \leq \bar{D}_d, 1 \leq j \leq \bar{M}_c}^\top$. This formulation provides a good trade-off between modeling accuracy and computational complexity. In particular, it allows us to reduce ϕ^m to the discrete feature representation ϕ^d when conditioned on a fixed assignment of continuous variables ϕ^c (and vice versa). This property is of central importance

³I.e., since modelling up to L -th order interactions of N variables requires $\sum_{l=0}^L \binom{N}{l} \in \mathcal{O}(N^L)$ terms.

for optimizing the acquisition function, as it allows us to optimize the mixed term of our model by leveraging the tools available for optimizing the discrete and continuous parts individually.

The proposed representation contains $M_m = M_d M_c$ features, thus resulting in a total of $M = M_d + M_c + M_d M_c$. To reduce model complexity, prior knowledge about the problem domain can be incorporated into the construction of the mixed features. In particular, one may consider the following approaches. Firstly, one can exploit a known interaction structure between variables, e.g., in form of a dependency graph, and ignore the features that are known to be irrelevant. Secondly, one can start by including all of the proposed pairwise feature combinations and progressively discard not-promising ones. Finally, for high-dimensional problems, one can use the opposite strategy and progressively add pairwise feature combinations, starting from the empty set.

3.2 Model Inference

Probabilistic Model Formulation. Let $\mathbf{X}_{1:t} \in \mathbb{R}^{t \times D}$ denote the matrix whose i^{th} row contains the input $\mathbf{x}_i \in \mathcal{X}$ queried at iteration i , $\dim \mathcal{X} = D$, and let $\mathbf{y}_{1:t} = [y_1, \dots, y_t]^\top \in \mathbb{R}^t$ denote the array containing the corresponding noisy function observations. Furthermore, let $\Phi_{1:t} \in \mathbb{R}^{t \times M}$ denote the matrix whose i^{th} row contains the featurized input $\phi(\mathbf{x}_i) \in \mathbb{R}^M$. Given the proposed formulation of f in Eq. (2) together with the noisy observation model, we obtain the Gaussian likelihood $p(\mathbf{y}_{1:t} | \mathbf{X}_{1:t}, \mathbf{w}) = \mathcal{N}(\Phi_{1:t} \mathbf{w}, \beta^{-1} \mathbf{I})$. To complete our model, we specify a prior distribution $p(\mathbf{w} | \alpha)$ over the coefficient vector \mathbf{w} parametrised by some scale parameter $\alpha > 0$. This prior should reflect our *a priori* knowledge about \mathbf{w} and thus the objective f . Given the likelihood and prior, the goal is to infer the posterior distribution $p(\mathbf{w} | \mathbf{X}_{1:t}, \mathbf{y}_{1:t}, \alpha, \beta) \propto p(\mathbf{y}_{1:t} | \mathbf{X}_{1:t}, \mathbf{w}, \beta) p(\mathbf{w} | \alpha)$. The difficulty of this crucially depends on the choice of prior, for which we present two viable alternatives.

Gaussian Prior. One natural way to complete a Gaussian likelihood model is to employ a zero-mean isotropic Gaussian prior distribution on the weight vector \mathbf{w} , i.e., $p(\mathbf{w} | \alpha) = \mathcal{N}(\mathbf{0}, \alpha^{-1} \mathbf{I})$, with precision $\alpha > 0$. A Gaussian prior encourages the weights to be uniformly small in size, so that the final predictor is a sum of many (or all) features, with each giving a small but non-zero contribution. Due to conjugacy, a Bayesian treatment of the weights \mathbf{w} yields a Gaussian posterior distribution $p(\mathbf{w} | \mathbf{X}_{1:t}, \mathbf{y}_{1:t}) = \mathcal{N}(\mathbf{m}, \mathbf{S}^{-1})$ with mean $\mathbf{m} = \beta \mathbf{S}^{-1} \Phi_{1:t}^\top \mathbf{y}_{1:t} \in \mathbb{R}^M$ and inverse covariance $\mathbf{S} = \alpha \mathbf{I} + \beta \Phi_{1:t}^\top \Phi_{1:t} \in \mathbb{R}^{M \times M}$ [8]. This simple analytical treatment of the posterior is a main benefit of this model, which can be viewed as a GP with a linear kernel in feature space.

Sparse Prior. While the number and degree of the features used in the model is a design choice, in practice it is typically unknown which variable interactions matter and thus which features to choose. To discard irrelevant features, one may impose a sparsity-encouraging prior over the weight vector \mathbf{w} [4]. However, due to non-conjugacy to the Gaussian likelihood, exact Bayesian inference of the resulting posterior distribution is in general intractable, inducing the need for approximate inference methods. One choice for such a prior is the Laplace distribution, for which approximate inference techniques based on expectation propagation [36] and variational inference [61] were developed in [52, 53, 54]. Alternatively, one can use a horseshoe prior and use Gibbs sampling to sample from the posterior over weights [4]. However, this comes with a significantly larger computational burden, which is a well-known issue for sampling based inference techniques [8]. Lastly, one may consider a spike-and-slab prior with expectation propagation for approximate posterior inference [21, 22].

3.3 Acquisition Function

We propose to use Thompson sampling (TS) [59], a technique which samples weights $\tilde{\mathbf{w}} \sim p(\mathbf{w} | \mathbf{X}_{1:t}, \mathbf{y}_{1:t}, \alpha, \beta)$ from the posterior distribution and chooses the next input by solving $\hat{\mathbf{x}} \in \arg \max_{\mathbf{x} \in \mathcal{X}} \tilde{\mathbf{w}}^\top \phi(\mathbf{x})$ (see Algorithm 1 in Appendix C). Intuitively, by sampling from the posterior, TS focuses on inputs that are plausibly optimal rather than those that are unlikely to be optimal.

TS has previously been successfully applied in both discrete and continuous domains [4, 38]. In addition, the following considerations make TS an ideal acquisition function for our problem. Firstly, the simple relation between the surrogate model and the resulting optimization problem for the acquisition function allows us to trade off model expressiveness and optimization tractability, which is a key challenge in mixed-variable domains. In particular, if we model second-order discrete interactions, the optimization of the acquisition function requires us to solve a quadratic mixed integer program, which can be done using available solvers and which allows us to incorporate complex constraints on the discrete variables. Secondly, in combination with a linear surrogate model it al-

lows us to provide a convergence analysis, making MiVABO the first mixed-variable BO method that enjoys theoretical guarantees.

Our acquisition strategy requires solving $\hat{\mathbf{x}} \in \arg \max_{\mathbf{x} \in \mathcal{X}} \tilde{\mathbf{w}}_t^\top \phi(\mathbf{x})$, which is a challenging mixed-variable optimization problem. To this end, we propose two schemes – alternating optimization and dual decomposition – which leverage independent subroutines for discrete and continuous optimization. While alternating optimization is a simple and efficient method that often works well in practice, dual decomposition comes with theoretical guarantees but is more expensive to run. Thus, in practice, one can choose the method to use based on the requirements of one’s application.

For the discrete part, we exploit of the fact that the optimization of a second-order pseudo-Boolean function can be formulated as a binary integer quadratic program (IQP) [9], allowing us to exploit commonly-used efficient and robust optimization tools, such as Gurobi [43] or CPLEX [26].⁴ This approach allows us to use any functionality offered by these solvers, such as the ability to optimize objectives subject to linear constraints $\mathbf{A}\mathbf{x}^d \leq \mathbf{b}$, $\mathbf{A} \in \mathbb{R}^{K \times D_d}$, $\mathbf{b} \in \mathbb{R}^K$ or quadratic constraints $\mathbf{x}^d^\top \mathbf{Q}\mathbf{x}^d + \mathbf{q}^\top \mathbf{x}^d \leq b$, $\mathbf{Q} \in \mathbb{R}^{D_d \times D_d}$, $\mathbf{q} \in \mathbb{R}^{D_d}$, $b \in \mathbb{R}$. For the continuous part, one can use optimizers commonly used in continuous BO, such as L-BFGS [35] or DIRECT [28].

Alternating Optimization. One natural way to optimize an objective in Eq. (2) is an alternating optimization scheme which iterates between optimizing the discrete variables \mathbf{x}^d conditioned on a particular setting of the continuous variables \mathbf{x}^c and vice versa, until convergence to some local optimum. While these approaches often provide no theoretical guarantees, they are widely applied in many contexts where the objective function is hard to optimize. In particular, we iteratively solve $\hat{\mathbf{x}}^d \in \arg \max_{\mathbf{x}^d \in \mathcal{X}^d} (\tilde{\mathbf{w}}^d^\top \phi^d(\mathbf{x}^d) + \tilde{\mathbf{w}}^m^\top \phi^m(\mathbf{x}^d, \mathbf{x}^c = \tilde{\mathbf{x}}^c))$ on the discrete domain and $\hat{\mathbf{x}}^c \in \arg \max_{\mathbf{x}^c \in \mathcal{X}^c} (\tilde{\mathbf{w}}^c^\top \phi^c(\mathbf{x}^c) + \tilde{\mathbf{w}}^m^\top \phi^m(\mathbf{x}^d = \tilde{\mathbf{x}}^d, \mathbf{x}^c))$ on the continuous domain. Importantly, the mixed features from Section 3.1 reduce these maximization problems to those that can be optimized by the oracles for discrete and continuous optimization.

Optimization with theoretical guarantees. Alternatively, one can maximize Eq. (2) using dual decomposition, which is a powerful approach based on Lagrangian optimization and has been successfully used for many problems [31, 57, 50]. Its well-studied theoretical properties facilitate the convergence analysis of MiVABO, making it particularly useful for settings where optimization accuracy is of crucial importance. Due to lack of space, we refer the reader to Appendix D for details on the dual decomposition and its derivation for our problem.

3.4 Convergence Analysis

The choice of a linear model and Thompson sampling allows us to leverage convergence analysis from linearly parameterized multi-armed bandits, which are a well-studied class of methods for solving structured decision making problems [1, 2]. As in our setting, these methods assume the objective to be a linear function of features $\phi(\mathbf{x}) \in \mathbb{R}^M$ with a fixed but unknown parameter vector $\mathbf{w} \in \mathbb{R}^M$, i.e. $\mathbb{E}[f(\mathbf{x})|\phi(\mathbf{x})] = \mathbf{w}^\top \phi(\mathbf{x})$, and aim at minimizing the *total regret* up to time T : $\mathcal{R}(T) = \sum_{t=1}^T (f(\mathbf{x}_*) - f(\mathbf{x}_t))$. We obtain the following probabilistic regret bound for MiVABO:

Proposition 1 *Assume that the following assumptions hold in every iteration $t = 1, \dots, T$:*

1. $\|\mathbf{w}_t\|_2 \leq c$, $\|\phi(\mathbf{x}_t)\|_2 \leq c$, $\|f(\mathbf{x}_*) - f(\mathbf{x}_t)\|_2 \leq c$, for some $c \in \mathbb{R}^+$.
2. $\mathbf{x}_t = \arg \max_{\mathbf{x}} \tilde{\mathbf{w}}^\top \phi(\mathbf{x})$ is selected exactly.⁵
3. $\tilde{\mathbf{w}}_t \sim \mathcal{N}(\mathbf{m}, 24M \ln T \ln \frac{1}{\delta} \mathbf{S}^{-1})$, i.e., the posterior variance \mathbf{S}^{-1} is scaled accordingly.

Then, the total regret of MiVABO is bounded by $\mathcal{R}(T) \leq \tilde{\mathcal{O}}\left(M^{3/2} \sqrt{T} \ln \frac{1}{\delta}\right)$ with probability $1 - \delta$.

Proposition 1 follows directly from Theorem 1 in [2] and is applicable to an infinite number of arms/inputs, i.e. where $\mathbf{x} \in \mathcal{X}$, $|\mathcal{X}| = \infty$. Proposition 1 implies *no-regret*, $\lim_{T \rightarrow \infty} \mathcal{R}(T)/T = 0$,

⁴While solving general binary IQPs is well-known to be NP-hard [9], these solvers are in practice very efficient for the problem dimensionalities we consider (i.e., with $D_d < 100$).

⁵Note that while this is not generally true for alternating optimization, it is guaranteed for dual decomposition under certain conditions.

i.e. convergence to the global maximum, since the maximum found after T iterations is no further away from $f(\mathbf{x}_*)$ than the average regret $\mathcal{R}(T)/T$. To the best of our knowledge, MiVaBO is the first mixed-variable BO algorithm for which such a guarantee is known to hold.

4 Experiments

We here present experimental results on tuning the hyperparameters of two machine learning algorithms, namely gradient boosting and a deep generative model. Further results can be found in Appendix A.

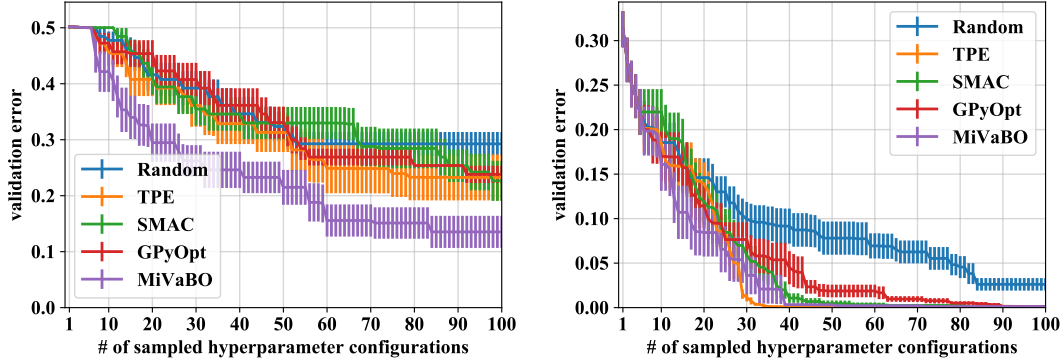


Figure 1: **XGBoost hyperparameter tuning.** Results on the datasets `monks-problem-1` (left) and `steel-plates-fault` (right). Mean plus/minus one standard deviation of the validation error over 16 random initializations. One can observe that MiVaBO significantly outperforms the competing state-of-the-art methods on the first dataset, while being competitive on the second.

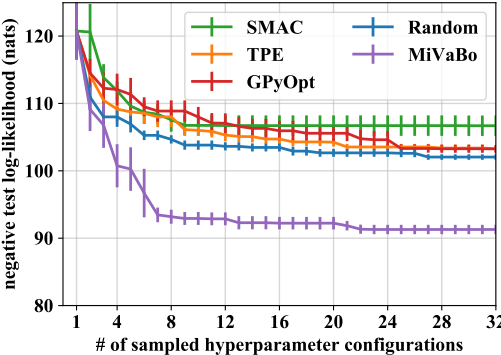


Figure 2: **VAE hyperparameter tuning on MNIST.** (left) Mean plus/minus one standard deviation of the negative test log-likelihood (NLL) in nats, estimated using 32 importance samples, over 8 random initializations. Every model was trained for 32 epochs. MiVaBO significantly outperforms the competing state-of-the-art methods, demonstrating its ability to handle the complex constrained nature of the VAE’s parameter space. Vertical axis starts from 80 nats for readability. (right) For the best models found by each algorithm in (left) after 32 BO iterations, we report their achieved NLL (in nats), estimated using 5000 importance samples, after training them for 3280 epochs. For convenience, we also report the NLL achieved after 32 training epochs, as plotted in (left).

MiVaBO. For the continuous model part, we employ Random Fourier Features (RFFs) approximating a GP with a squared exponential (SE) kernel, as we found RFFs to provide the best trade-off between complexity and accuracy in practice. We use the alternating optimization scheme for Thompson sampling, which we always run until convergence to a local optimum. We use Gurobi [43] as the discrete optimization oracle, and L-BFGS [35] as the continuous optimization oracle. We did not tune any parameters, but left the prior variance α , observation noise variance β , and

kernel bandwidth σ at 1.0, and scaled the posterior variance by the factor stated in Proposition 1. We impose a Gaussian prior over the weights, allowing us to perform closed-form inference. While, in our experiments, a sparse prior often yielded better results, this marginal performance gain came with the significantly increased computational effort required to approximate the posterior.

Baselines. We compare against four baselines: SMAC [25], TPE [7], random search [6], and the popular GPyOpt open-source BO Python package [17]. GPyOpt is based on a Gaussian process (GP) model, which constitutes the most commonly used approach in practice. To account for mixed variable types, GPyOpt relaxes discrete variables to be continuous and later rounds them to the nearest discrete neighbor. We use SMAC, TPE and GPyOpt with their respective default settings.⁶

Results for gradient boosting hyperparameter tuning. We use the publicly available OpenML database [60], which contains evaluations for various machine learning methods trained on several datasets with many hyperparameter settings. We consider one of the most popular algorithms from OpenML (in terms of number of evaluations), namely XGBoost, which is an efficient implementation of the extreme gradient boosting framework from [11]. The task is to tune its ten hyperparameters (of which three are discrete and seven continuous) as to minimize the classification error on a held-out test set after being trained. We consider two different datasets, each containing more than 45000 hyperparameter evaluations. See Appendix F for more details on XGBoost and the datasets used. To evaluate settings for which no data is available, we use a surrogate modeling approach [13] based on nearest neighbor; i.e., for a given hyperparameter setting, the objective returns the error of the closest (in terms of Euclidean distance) setting available in the database. The results in Fig. 1 show that MIVABO achieves performance which is either significantly stronger than (left plot) or competitive with (right plot) the state-of-the-art mixed-variable BO algorithms on this challenging task (depending on the dataset used for evaluation). GPyOpt performs poorly, which is likely due to the fact that it cannot account for the discrete variables in a principled way. As compared to TPE and SMAC, our method likely benefits from more sophisticated uncertainty estimation.

Results for deep generative model hyperparameter tuning. Deep generative models have recently received considerable attention in the machine learning community. Despite their popularity and importance, effectively tuning their hyperparameters is a major challenge, which is partly due to the increasing complexity of their deep neural network based architectures. We consider the task of tuning the hyperparameters of a variational auto-encoder (VAE) [29, 48] composed of a convolutional encoder and a deconvolutional decoder, as, e.g., considered in [12, 51]. The VAEs are evaluated on the standard train/test split of the stochastically binarized version of the MNIST handwritten digits dataset [33], as, e.g., considered in [10, 47]. The models are trained on 60000 images for 32 epochs, using stochastic gradient descent with a mini-batch size of 128. As an error metric, we report the negative log-likelihood (in nats) achieved by the VAEs on a held-out test set of 10000 images, as estimated via importance sampling [48] using 32 importance samples per test point. To the best of our knowledge, this is the first BO paper that considers tuning a deep generative model.

Tuning this model is difficult due to the high-dimensional and structured nature of its hyperparameter space, and in particular due to various constraints arising from mutual dependencies between certain parameters. We tune 25 discrete parameters defining the model architecture, including the number of convolutional and fully-connected layers, layer-specific parameters such as stride, padding and filter size (for convolutional layers) or number of units (for fully-connected layers), as well as the dimensionality of the VAE’s latent space. We furthermore tune four continuous parameters controlling the optimizer and regularization. Crucially, the discrete parameters exhibit mutual dependencies which result in complex constraints in hyperparameter space, as certain combinations of stride, padding and filter size lead to invalid architectures both for the encoder, where the shapes of all layers must be integral, and for the decoder, where the shape of the final output layer needs to match the shape of the input data (due to the VAE’s autoencoding nature), i.e. one channel of size 28×28 for MNIST. The latter constraint is particularly challenging, as only a small number of possible decoder configurations yield the required output shape. See Appendix B for more details on this experiment.

While MIVABO can conveniently capture these restrictions via linear and quadratic constraints in hyperparameter space, the competing methods cannot, which makes a fair comparison difficult. We thus adapt the other methods to handle constraints as follows: If a method tries to evaluate an invalid

⁶See Appendix F for details on the implementations we used. Since we do not consider settings where cheap approximations of the objective are available, we cannot compare against HB or BOHB.

parameter configuration, we simply return a penalty error value, which will discourage a model-based method to sample this (or a similar) setting again in the future. However, for fairness, we only report valid observations and ignore all configurations that violated a constraint. We set the penalty value to 500 nats, which corresponds to the error a uniformly random generator incurs.⁷

The results are presented in Fig. 2. It can be seen from the plot in Fig. 2 (left) that MiVABO significantly outperforms the competing methods on this task. This is because MiVABO is able to naturally encode the constraints and thus to directly optimize over the feasible region in parameter space, while TPE, SMAC and GPyOpt need to learn the constraints from data. They fail to do so and get stuck in bad local optima early on. The model-based approaches likely have difficulties due to sharp discontinuities in hyperparameter space induced by the constraint violation penalties (i.e., as invalid configurations may lie close to well-performing configurations). In contrast, random search is agnostic to these discontinuities, and thus notably outperforms the model-based methods.

Finally, Fig. 2 (right) shows that the best VAE architecture found by MiVABO achieves 84.25 nats when trained for 3280 epochs and using 5000 importance samples for test log-likelihood estimation (which is the number of epochs and importance samples used in [10]). This is comparable to the performance achieved by models tuned by human experts, as e.g. reported in [51]. While our result is not entirely comparable with the one in [51] (e.g., in [51], they use three (de-)convolutional layers, and a more sophisticated inference procedure than a standard VAE), this indicates the potential usefulness of MiVABO in tuning deep generative models parameterized by convolutional architectures, especially when noting the significantly worse performance of the competing BO approaches.⁸

5 Conclusion

We propose MiVABO, a simple yet effective method for efficient optimization of expensive-to-evaluate mixed-variable black-box objective functions, combining a linear model of expressive features with Thompson sampling. Our method is characterized by a high degree of flexibility due to the modularity of its components, i.e., the feature mapping used to model the mixed-input objective, and the optimization oracles used as subroutines for the acquisition procedure. This allows practitioners to tailor MiVABO to specific objectives, e.g. by incorporating prior knowledge in the feature design or by exploiting optimization oracles that can handle specific types of constraints. Moreover, we show that MiVABO enjoys strong theoretical convergence guarantees that competing methods lack. Finally, we empirically demonstrate that MiVABO significantly improves optimization performance as compared to state-of-the-art data driven methods for mixed-variable optimization.

Acknowledgements

This research has been partially supported by SNSF NFP75 grant 407540_167189. Matteo Turchetta was supported through the ETH-MPI Center for Learning Systems. The authors would like to thank Josip Djolonga, Mojmír Mutný, Johannes Kirschner, Alonso Marco Valle, David R. Burt, Ross Clarke, Wolfgang Roth as well as the anonymous reviewers of an earlier version of this paper for their helpful feedback.

References

- [1] Marc Abeille, Alessandro Lazaric, et al. Linear Thompson sampling revisited. *Electronic Journal of Statistics*, 2017.
- [2] Shipra Agrawal and Navin Goyal. Thompson sampling for contextual bandits with linear payoffs. In *International conference on Machine learning (ICML)*, 2013.
- [3] Lukáš Bajer and Martin Holeňa. Surrogate model for continuous and discrete genetic optimization based on rbf networks. In *Proceedings of the 11th International Conference on Intelligent Data Engineering and Automated Learning*, 2010.

⁷Note that the penalty value does not qualitatively affect the reported results, as shown in Appendix B.3.

⁸Fig. 2 (right) also shows that the relative performance differences between the competing methods after only 32 training epochs provide a reasonable proxy for the performance differences after 3280 training epochs. This observation helped us to significantly speed up the model tuning process (i.e., by around 100 \times).

- [4] Ricardo Baptista and Matthias Poloczek. Bayesian optimization of combinatorial structures. *arXiv preprint arXiv:1806.08838*, 2018.
- [5] James Bergstra, Rémi Bardenet, B Kégl, and Y Bengio. Implementations of algorithms for hyper-parameter optimization. In *NIPS Workshop on Bayesian optimization*, 2011.
- [6] James Bergstra and Yoshua Bengio. Random search for hyper-parameter optimization. *Journal of Machine Learning Research*, 13(Feb):281–305, 2012.
- [7] James S Bergstra, Rémi Bardenet, Yoshua Bengio, and Balázs Kégl. Algorithms for hyper-parameter optimization. In *Advances in Neural Information Processing Systems (NIPS)*, 2011.
- [8] Christopher M Bishop. *Pattern recognition and machine learning*. Springer, 2006.
- [9] Endre Boros and Peter L Hammer. Pseudo-boolean optimization. *Discrete applied mathematics*, 123(1-3):155–225, 2002.
- [10] Yuri Burda, Roger Grosse, and Ruslan Salakhutdinov. Importance weighted autoencoders. *arXiv preprint arXiv:1509.00519*, 2015.
- [11] Tianqi Chen and Carlos Guestrin. Xgboost: A scalable tree boosting system. In *International Conference on Knowledge Discovery and Data Mining*, 2016.
- [12] Alexey Dosovitskiy, Jost Tobias Springenberg, and Thomas Brox. Learning to generate chairs with convolutional neural networks. In *Proceedings of the IEEE Conference on Computer Vision and Pattern Recognition*, pages 1538–1546, 2015.
- [13] Katharina Eggensperger, Frank Hutter, Holger H Hoos, and Kevin Leyton-Brown. Efficient benchmarking of hyperparameter optimizers via surrogates. In *AAAI*, pages 1114–1120, 2015.
- [14] Stefan Falkner, Aaron Klein, and Frank Hutter. BOHB: Robust and efficient hyperparameter optimization at scale. *arXiv preprint arXiv:1807.01774*, 2018.
- [15] Eduardo C. Garrido-Merchán and Daniel Hernández-Lobato. Dealing with categorical and integer-valued variables in bayesian optimization with gaussian processes. *CoRR*, 2018.
- [16] Andrew Gelman, John B Carlin, Hal S Stern, and Donald B Rubin. *Bayesian data analysis*. Chapman and Hall/CRC, 1995.
- [17] J González. GPyOpt: A Bayesian optimization framework in Python, 2016.
- [18] Trevor J Hastie. Generalized additive models. In *Statistical models in S*, pages 249–307. Routledge, 2017.
- [19] Elad Hazan, Adam Klivans, and Yang Yuan. Hyperparameter optimization: A spectral approach. *arXiv preprint arXiv:1706.00764*, 2017.
- [20] P. Hennig and C. J. Schuler. Entropy search for information-efficient global optimization. *JMLR*, 13:1809–1837, 2012.
- [21] Daniel Hernández-Lobato, José Miguel Hernández-Lobato, and Pierre Dupont. Generalized spike-and-slab priors for bayesian group feature selection using expectation propagation. *The Journal of Machine Learning Research*, 14(1):1891–1945, 2013.
- [22] José Miguel Hernández-Lobato, Daniel Hernández-Lobato, and Alberto Suárez. Expectation propagation in linear regression models with spike-and-slab priors. *Machine Learning*, 99(3):437–487, 2015.
- [23] Trong Nghia Hoang, Quang Minh Hoang, Ruofei Ouyang, and Kian Hsiang Low. Decentralized high-dimensional bayesian optimization with factor graphs. In *Thirty-Second AAAI Conference on Artificial Intelligence*, 2018.
- [24] Frank Hutter, Holger H Hoos, and Kevin Leyton-Brown. Automated configuration of mixed integer programming solvers. In *International Conference on Integration of Artificial Intelligence (AI) and Operations Research (OR) Techniques in Constraint Programming*, 2010.
- [25] Frank Hutter, Holger H Hoos, and Kevin Leyton-Brown. Sequential model-based optimization for general algorithm configuration. In *International Conference on Learning and Intelligent Optimization*, pages 507–523. Springer, 2011.
- [26] IBM. Users manual for CPLEX. *International Business Machines Corporation*, 46(53):157, 2009.

[27] Rodolphe Jenatton, Cedric Archambeau, Javier González, and Matthias Seeger. Bayesian optimization with tree-structured dependencies. In *International Conference on Machine Learning (ICML)*, 2017.

[28] Donald R. Jones. Direct global optimization algorithm. *Encyclopedia of Optimization*, 2001.

[29] Diederik P Kingma and Max Welling. Auto-encoding variational bayes. *arXiv preprint arXiv:1312.6114*, 2013.

[30] Daphne Koller, Nir Friedman, and Francis Bach. *Probabilistic graphical models: principles and techniques*. MIT press, 2009.

[31] Nikos Komodakis, Nikos Paragios, and Georgios Tziritas. MRF energy minimization and beyond via dual decomposition. *IEEE transactions on pattern analysis and machine intelligence*, 2011.

[32] Andreas Krause, Ajit Singh, and Carlos Guestrin. Near-optimal sensor placements in Gaussian processes: Theory, efficient algorithms and empirical studies. *Journal of Machine Learning Research*, 2008.

[33] Yann LeCun, Corinna Cortes, and CJ Burges. Mnist handwritten digit database. *AT&T Labs [Online]. Available: http://yann. lecun. com/exdb/minst*, 2:18, 2010.

[34] Lisha Li, Kevin Jamieson, Giulia DeSalvo, Afshin Rostamizadeh, and Ameet Talwalkar. Hyperband: A novel bandit-based approach to hyperparameter optimization. *arXiv preprint arXiv:1603.06560*, 2016.

[35] Dong C Liu and Jorge Nocedal. On the limited memory BFGS method for large scale optimization. *Mathematical programming*, 45(1-3):503–528, 1989.

[36] Thomas P Minka. Expectation propagation for approximate Bayesian inference. In *UAI*, pages 362–369, 2001.

[37] Jonas Mockus. On Bayesian methods for seeking the extremum. In *Optimization Techniques IFIP Technical Conference*, pages 400–404. Springer, 1975.

[38] Mojmir Mutný and Andreas Krause. Efficient high dimensional bayesian optimization with additivity and quadrature fourier features. In *Advances in Neural Information Processing Systems (NIPS)*, December 2018.

[39] Diana M Negoescu, Peter I Frazier, and Warren B Powell. The knowledge-gradient algorithm for sequencing experiments in drug discovery. *INFORMS Journal on Computing*, 2011.

[40] Hannes Nickisch. glm-ie: generalised linear models inference & estimation toolbox. *Journal of Machine Learning Research*, 13(May):1699–1703, 2012.

[41] Ryan O’Donnell. *Analysis of boolean functions*. Cambridge University Press, 2014.

[42] Changyong Oh, Jakub M. Tomczak, Efstratios Gavves, and Max Welling. Combinatorial bayesian optimization using graph representations. *arXiv preprint arXiv:1902.00448*, 2019.

[43] Gurobi Optimization. Gurobi optimizer reference manual. <http://www.gurobi.com>, 2014.

[44] Valerio Perrone, Rodolphe Jenatton, Matthias Seeger, and Cedric Archambeau. Multiple adaptive Bayesian linear regression for scalable bayesian optimization with warm start. *arXiv preprint arXiv:1712.02902*, 2017.

[45] Ali Rahimi and Benjamin Recht. Random features for large-scale kernel machines. In *Advances in Neural Information Processing Systems (NIPS)*, pages 1177–1184, 2008.

[46] Ali Rahimi and Benjamin Recht. Weighted sums of random kitchen sinks: Replacing minimization with randomization in learning. In *Advances in Neural Information Processing Systems (NIPS)*, 2009.

[47] Tom Rainforth, Adam R Kosiorek, Tuan Anh Le, Chris J Maddison, Maximilian Igl, Frank Wood, and Yee Whye Teh. Tighter variational bounds are not necessarily better. *arXiv preprint arXiv:1802.04537*, 2018.

[48] Danilo Jimenez Rezende, Shakir Mohamed, and Daan Wierstra. Stochastic backpropagation and approximate inference in deep generative models. *arXiv preprint arXiv:1401.4082*, 2014.

[49] Paul Rolland, Jonathan Scarlett, Ilija Bogunovic, and Volkan Cevher. High-dimensional Bayesian optimization via additive models with overlapping groups. *arXiv preprint arXiv:1802.07028*, 2018.

[50] Alexander M Rush and MJ Collins. A tutorial on dual decomposition and Lagrangian relaxation for inference in natural language processing. *Journal of Artificial Intelligence Research*, 45:305–362, 2012.

[51] Tim Salimans, Diederik P Kingma, and Max Welling. Markov chain monte carlo and variational inference: Bridging the gap. *arXiv preprint arXiv:1410.6460*, 2014.

[52] Matthias W Seeger. Bayesian inference and optimal design for the sparse linear model. *Journal of Machine Learning Research*, 9(Apr):759–813, 2008.

[53] Matthias W Seeger and Hannes Nickisch. Compressed sensing and bayesian experimental design. In *International Conference on Machine Learning (ICML)*. ACM, 2008.

[54] Matthias W Seeger and Hannes Nickisch. Large scale Bayesian inference and experimental design for sparse linear models. *SIAM Journal on Imaging Sciences*, 4(1):166–199, 2011.

[55] Bobak Shahriari, Kevin Swersky, Ziyu Wang, Ryan P. Adams, and Nando de Freitas. Taking the human out of the loop: A review of Bayesian optimization. *Proceedings of the IEEE*, 2016.

[56] Jasper Snoek, Oren Rippel, Kevin Swersky, Ryan Kiros, Nadathur Satish, Narayanan Sundaram, Mostofa Patwary, Mr Prabhat, and Ryan Adams. Scalable Bayesian optimization using deep neural networks. In *International Conference on Machine Learning (ICML)*, 2015.

[57] David Sontag, Amir Globerson, and Tommi Jaakkola. Introduction to dual composition for inference. In *Optimization for Machine Learning*. MIT Press, 2011.

[58] N. Srinivas, A. Krause, S. Kakade, and M. Seeger. Gaussian process optimization in the bandit setting: No regret and experimental design. In *International Conference on Machine Learning (ICML)*, 2010.

[59] William R Thompson. On the likelihood that one unknown probability exceeds another in view of the evidence of two samples. *Biometrika*, 1933.

[60] Joaquin Vanschoren, Jan N Van Rijn, Bernd Bischl, and Luis Torgo. Openml: networked science in machine learning. *ACM SIGKDD Explorations Newsletter*, 15(2):49–60, 2014.

[61] Martin J Wainwright, Michael I Jordan, et al. Graphical models, exponential families, and variational inference. *Foundations and Trends® in Machine Learning*, 1(1–2):1–305, 2008.

[62] Zi Wang and Stefanie Jegelka. Max-value entropy search for efficient bayesian optimization. In *International Conference on Machine Learning (ICML)*, 2017.

[63] Christopher KI Williams and Carl Edward Rasmussen. *Gaussian processes for machine learning*. MIT Press Cambridge, MA, 2006.

A Further Experimental Results

A.1 Synthetic Benchmark for Unconstrained Optimization

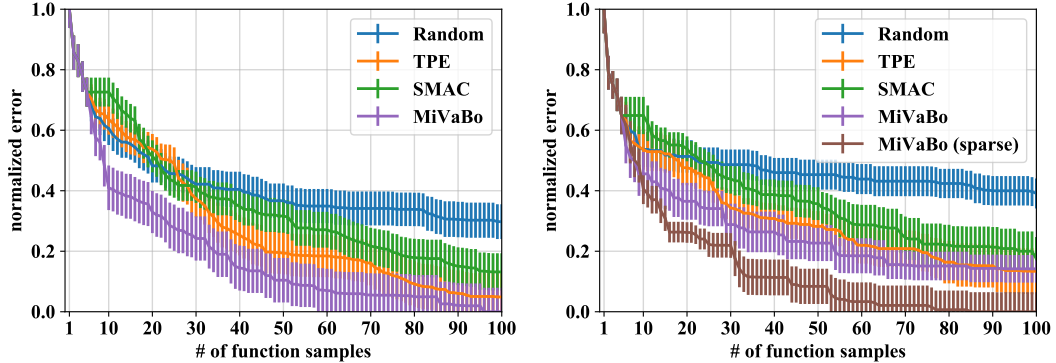


Figure 3: Results on the synthetic benchmark, with the Gaussian (left) and Laplace prior (right). Mean plus/minus one standard deviation of the normalized error over 16 random initializations. (Left) MiVaBo outperforms its competitors. (Right) MiVaBo with a sparse prior outperforms its competitors, including MiVaBo with a Gaussian prior

We assess the performance on an unconstrained synthetic linear benchmark function of the form $f(\mathbf{x}) = \mathbf{w}^\top \phi$. We choose a fairly high-dimensional objective with $D_d = 8$ discrete and $D_c = 8$ continuous variables, thus resulting in a total input space dimensionality of $D = D_d + D_c = 16$. For the discrete model part, we choose the $M_d \in \mathcal{O}(D_d^2)$ features ϕ^d proposed in Section 3.1. For the continuous features ϕ^c , we choose $M_c = 16$ dimensional Random Fourier Features to approximate a GP with a squared exponential kernel with bandwidth $\sigma = 1.0$. For the mixed representation, we construct a feature vector ϕ^m by stacking all pairs of discrete and continuous features, as proposed in Section 3.1. We consider two settings for the weight vector: Firstly, we sample it from a zero-mean Gaussian, $\mathbf{w} \sim \mathcal{N}(\mathbf{0}, \mathbf{I}) \in \mathbb{R}^M$. Secondly, we sample it from a Laplace distribution, i.e. $\mathbf{w} \sim p(\mathbf{w}|\alpha) \propto \exp(-\alpha^{-1}\|\mathbf{w}\|_1)$, with inverse scale parameter $\alpha = 0.1$, and then prune all weights smaller than 10 to zero to induce sparsity over the weight vector. For the second setting, we also assess MiVaBo using a Laplace prior and the approximate inference technique from [54].⁹ As we do not know the true optimum of the function and thus cannot compute the regret, we normalize all observed function values to the interval $[0, 1]$, resulting in a normalized error as the metric of comparison. We can observe from our results shown in Fig. 3 that MiVaBo outperforms the competing methods in this setting, demonstrating the effectiveness of our approach when its modeling assumptions are fulfilled.

A.2 Synthetic Benchmark for Constrained Optimization

In another experiment, we demonstrate the capability of our algorithm to incorporate linear constraints on the discrete variables. In particular, we want to enforce a solution that is sparse in the discrete variables via adding a hard cardinality constraint of the type $\sum_{i=1}^{D_d} x_i^d \leq k$, which we can simply specify in the Gurobi optimizer. Cardinality constraints of this type are very relevant in practice, as many real-world problems desire sparse solutions (e.g., sparsification of ising models, contamination control, aero-structural multi-component problems [4]). We consider the same functional form as before, i.e. again with $D_d = D_c = 8$, and set $k = 2$, meaning that a solution should have at most two of our binary variables set to one, while all others shall be set to zero. To enable comparison with TPE, SMAC and random search, which provide no capability of modeling these kinds of constraints, we assume the objective f to be unconstrained, but instead return a large penalty value if a method acquires an evaluation of f at a point that violates the constraint. Thus, the baseline algorithms are forced to learn the constraint from observations, which is a challenging problem.

⁹We use the MATLAB implementation provided in the `glm-ie` toolbox [40] by the same authors.

One can notice from Fig. 4 that the ability to explicitly encode the cardinality constraint into the discrete optimization oracle significantly increases performance.

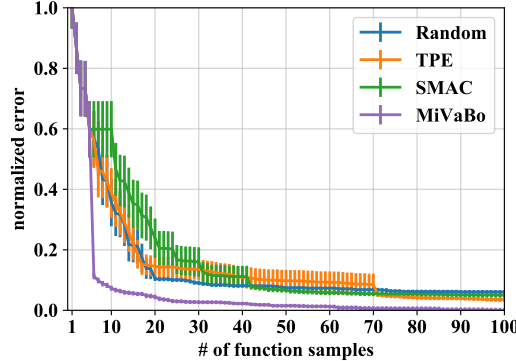


Figure 4: Results on the synthetic benchmark with cardinality constraints. The curves represent the mean plus/minus one standard deviation of the normalized error over 16 random initializations. One can observe that MiVaBo outperforms its competitors.

B More Details on VAE Hyperparameter Tuning Task

B.1 Hyperparameters of VAE

We used the PyTorch library to implement the VAE used in the experiment. Table 1 describes the names, types and domains of the involved hyperparameters that we tune. Whenever we refer to a "deconvolutional layer" (also called transposed convolution or fractionally-strided convolution), we mean the functional mapping implemented by a ConvTranspose2d layer in PyTorch¹⁰. Since our approach operates on a binary encoding of the discrete parameters, we also display the number of bits required to encode each discrete parameter. In total, we consider 25 discrete parameters (resulting in 50 when binarized) as well as 4 continuous ones.

B.2 Description of Constraints

We now describe the constraints arising from the mutual dependencies within the hyperparameter space of the deconvolutional VAE (as described in Appendix B.1).

Encoder constraints. For the convolutional layers (up to two in our case) of the encoder, we need to ensure that the chosen combination of stride, padding and filter size transforms the input image into an output image whose shape is integral (i.e., not fractional). More precisely, denoting the input image size by W_{in} (i.e., the input image is quadratic with shape $W_{\text{in}} \times W_{\text{in}}$), the stride by S , the filter size by F , and the padding by P , we need to ensure that the output image size W_{out} is integral, i.e.

$$W_{\text{out}}^e = (W_{\text{in}}^e - F^e + P^e) / S^e + 1 \in \mathbb{N} \quad (3)$$

where superscripts e are used to make clear that we are considering the encoder. Let us illustrate this with an example¹¹: For $W_{\text{in}} = 10$, $P = 0$, $S = 2$ and $F = 3$, we would get an invalid fractional output size of $W_{\text{out}} = (10 - 3 + 0)/2 + 1 = 4.5$. To obtain a valid output size, one could, e.g., instead consider a padding of $P = 1$, yielding $W_{\text{out}} = (10 - 3 + 1)/2 + 1 = 5$. Alternatively, one could also consider a stride of $S = 1$ to obtain $W_{\text{out}} = (10 - 3 + 0)/1 + 1 = 8$, or a filter size of $F = 4$ to obtain $W_{\text{out}} = (10 - 4 + 0)/2 + 1 = 4$ (though the latter is very uncommon and thus not allowed in our setting; we only allow $F \in \{3, 5\}$, as described in Appendix B.1). While this

¹⁰See <https://pytorch.org/docs/stable/nn.html#convtranspose2d> for details.

¹¹This example is taken from <http://cs231n.github.io/convolutional-networks/#conv> (paragraph "Constraints on strides"), which also describes the constraints discussed here. Note that they define the padding P in a slightly different way (i.e., they only consider symmetric padding, while we also allow for asymmetric padding) and thus end up with a term of $2P$ instead of P in the formula.

Table 1: **Hyperparameters of the VAE.** The architecture of the VAE (if all layers are enabled) is C1–C2–F1–F2–z–F3–F4–D1–D2, with C denoting a convolutional (conv.) layer, F a fully-connected (fc.) layer, D a deconvolutional (deconv.) layer and z the latent space. Layers F2 and F3 have fixed sizes of $2d_z$ and d_z units respectively, where d_z denotes the dimensionality of the latent space z. The domain of the number of units of the fc. layers F1 and F4 is discretized with a step size of 64, i.e. $[0, 64, 128, \dots, 832, 896, 960]$, denoted by $[0 \dots 960]$ in the table for brevity. For d_z , the domain $[16 \dots 64]$ refers to all integers within that interval.

#	Name	Type	Domain	Bits
1	Number of conv. layers in encoder	discrete	$[0,1,2]$	2
	Parameters of C1			
2	Number of channels of C1	discrete	$[4,8,16,24]$	2
3	Stride of C1	discrete	$[1,2]$	1
4	Filter size of C1	discrete	$[3,5]$	1
5	Padding of C1	discrete	$[0,1,2,3]$	2
	Parameters of C2			
6	Number of channels of C2	discrete	$[8,16,32,48]$	2
7	Stride of C2	discrete	$[1,2]$	1
8	Filter size of C2	discrete	$[3,5]$	1
9	Padding of C2	discrete	$[0,1,2,3]$	2
10	Number of fc. layers in encoder	discrete	$[0,1,2]$	2
11	Number of units of F1	discrete	$[0 \dots 960]$	4
12	Dimensionality d_z of z	discrete	$[16 \dots 64]$	6
13	Number of fc. layers in decoder	discrete	$[0,1,2]$	2
14	Number of units of F4	discrete	$[0 \dots 960]$	4
15	Number of deconv. layers in decoder	discrete	$[0,1,2]$	2
	Parameters of D1			
16	Number of channels of D1	discrete	$[8,16,32,48]$	2
17	Stride of D1	discrete	$[1,2]$	1
18	Filter size of D1	discrete	$[3,5]$	1
19	Padding of D1	discrete	$[0,1,2,3]$	2
20	Output padding of D1	discrete	$[0,1,2,3]$	2
	Parameters of D2			
21	Number of channels of D2	discrete	$[4,8,16,24]$	2
22	Stride of D2	discrete	$[1,2]$	1
23	Filter size of D2	discrete	$[3,5]$	1
24	Padding of D2	discrete	$[0,1,2,3]$	2
25	Output padding of D2	discrete	$[0,1,2,3]$	2
26	Learning rate	continuous	$[10^{-4}, 10^{-2}]$	-
27	Momentum	continuous	$[0.1, 0.5]$	-
28	Learning rate decay factor	continuous	$[0.5, 1.0]$	-
29	Weight decay regularization	continuous	$[10^{-6}, 10^{-2}]$	-
	Total			50

constraint is not trivially fulfilled (which can be verified by manually trying different configurations of W_{in} , F , S , P), it is also not too challenging to find valid configurations.

Note that this constraint is required to be fulfilled for every convolutional layer; we thus obtain the following two constraints in our specific two-layer setting, where $W_{\text{in}} = 28$ (as MNIST images are of shape 28×28):

$$W_{\text{out}1}^e = (28 - F_1^e + P_1^e)/S_1^e + 1 \quad \in \mathbb{N}, \quad (4)$$

$$W_{\text{out}2}^e = (W_{\text{out}1}^e - F_2^e + P_2^e)/S_2^e + 1 \quad \in \mathbb{N}. \quad (5)$$

where the subscripts in $\{1, 2\}$ denote the index of the convolutional layer.

Finally, observe that the constraints in Eq. (4) and Eq. (5) are, respectively, linear and quadratic in the discrete variables $F_1^e, F_2^e, P_1^e, P_2^e, S_1^e, S_2^e$, and can thus be readily incorporated into the inte-

ger programming solver (e.g. Gurobi [43] or CPLEX [26]) we employ as a subroutine within our acquisition function optimization strategy.

Decoder constraints. While the constraints on the decoder architecture are similar in nature to those for the encoder, they are significantly more difficult to fulfill, which we will now illustrate.

In particular, we need to ensure that the decoder produces images of shape 28×28 . By inverting the formula in Eq. (3), we see that for a deconvolutional layer (which intuitively implements an inversion of the convolution operation), the output image size W_{out} can be computed as

$$W_{\text{out}}^d = (W_{\text{in}}^d - 1) \times S^d + F^d - 2P^d + O^d \quad (6)$$

where superscripts d are used to make clear that we are considering the decoder, and where O is an additional output padding parameter which can be used to adjust the shape of the output image¹². Note that we now have a factor of $2P$ in Eq. (6) instead of P (as for the encoder, i.e. in Eq. (3)), since we only consider symmetric padding for the decoder, why we allow for asymmetric padding for the encoder (to make it easier to fulfill the integrality constraints for the encoder due to an increased number of valid configurations). The output padding parameter O is required since the mapping from W_{in}^e to W_{out}^e in a convolutional layer (i.e. in the encoder) is not bijective: there are different combinations of W_{in}^e, F, S, P that result in the same W_{out}^e (which can be easily verified). Thus, given an output size W_{out}^e (now serving as the input size W_{in}^d of the deconvolutional layer), there is no unique corresponding input size W_{in}^e (now serving as the output size W_{out}^d of the deconvolutional layer). The output padding parameter O can thus be used to disambiguate this relation. Note that W_{out}^d in Eq. (6) is always integral, so there are no integrality constraints involved here, in contrast to the encoder.

In the context of our decoder model, i.e. with up to two deconvolutional layers, and with a required output image size of 28, we thus obtain the following constraints:

$$W_{\text{out}}^d = (W_{\text{in}}^d - 1) \times S_1^d + F_1^d - 2P_1^d + O_1^d, \quad (7)$$

$$28 = (W_{\text{out}}^d - 1) \times S_2^d + F_2^d - 2P_2^d + O_2^d, \quad (8)$$

i.e. we need to choose the parameters $F_1^d, F_2^d, P_1^d, P_2^d, S_1^d, S_2^d, O_1^d, O_2^d$ such that the output size is 28, which is challenging, as only a small number of parameter configurations fulfill this property. While this problem is already challenging when assuming a given fixed input image shape W_{in}^d , in our setting it is more difficult, as W_{in}^d has to be of a suitable size as well. Note that W_{in}^d is determined by the size of the fully-connected layer preceding the first deconvolutional layer, which yields an additional challenge: the size of the last fully-connected layer has to be set such that it can be resized to an image of shape $C_1^d \times W_{\text{in}}^d \times W_{\text{in}}^d$ (i.e., such that it can be fed into a deconvolutional layer), where C_1^d denotes the number of channels of the first deconvolutional layer of the decoder. As the resulting problem would be too challenging for any algorithm to produce a valid solution in a reasonable amount of time, we simplify it slightly by only treating C_1^d as a design parameter (as described in Appendix B.1), but keeping $W_{\text{in}}^d = 7$ fixed. The value 7 is chosen since $16 \times 7 \times 7 = 784$, i.e., when setting $C_1^d = 16$, the last fully-connected layer has the correct output shape (since $28 \times 28 = 784$ for an MNIST image). This way, a valid decoder architecture can be achieved by deactivating all convolutional layers and choosing $C_1^d = 16$, constituting an alternative if fulfilling the decoder constraints in Eq. (7) and Eq. (8) is too challenging for an algorithm.

Finally, the constraints in Eq. (7) and Eq. (8) are, respectively, linear and quadratic in the discrete variables $F_1^d, F_2^d, P_1^d, P_2^d, S_1^d, S_2^d, O_1^d, O_2^d$, which again allows us to incorporate them into our optimization routine.

B.3 Effect of Different Constraint Violation Penalty Values

We now analyze the effect of the constraint violation penalty value on the performance of SMAC, TPE and GPyOpt. Note that random search and MiVABO are not affected by the penalty. We do this analysis to show that the choice of penalty does not qualitatively affect the reported results. In addition to the penalty of 500 nats considered in the experiments in the main paper, we assessed

¹²See e.g. <https://pytorch.org/docs/stable/nn.html#convtranspose2d> for a description of the output padding in the context of the PyTorch library we use.

two smaller alternative penalties of 250 nats and 125 nats, respectively. The results in Table 2 show that the performance of the methods improves marginally with decreasing penalty values. This can be intuitively explained by the fact that the smaller the penalty, the smaller the region in hyperparameter space that the penalty discourages from searching. I.e., a large penalty may not only discourage infeasible configurations, but also feasible configurations that lie “close” to the penalized infeasible one (where closeness is defined by the specific surrogate model employed by the method). However, even for the smallest penalty of 125 nats, SMAC, TPE and GPyOpt still perform worse than random search, and thus still significantly worse than MiVABO. Imposing penalties that are significantly smaller than 125 is not sensible, as this will encourage the model-based methods to violate the constraints, and in turn discourage them from ever evaluating a valid configuration (as this would yield a worse score).

Finally, Table 3 shows the number of constraint violations by the different methods, depending on the violation penalty.

Table 2: Mean plus/minus one standard deviation of the negative test log-likelihood over 8 random initializations, achieved by the best VAE configuration found by SMAC, TPE and GPyOpt after 16 BO iterations, for constraint violation penalties of 500, 250 and 125 nats. Performance values of MiVABO and random search (which are not affected by the penalty) are included for reference.

Algorithm	Penalty (nats)		
	500	250	125
SMAC	112.96 \pm 1.79	112.08 \pm 1.77	111.06 \pm 1.57
TPE	108.77 \pm 1.22	108.10 \pm 1.26	108.09 \pm 1.26
GPyOpt	108.53 \pm 1.09	108.53 \pm 0.57	106.52 \pm 1.40
Random search			106.35 \pm 0.86
MiVABO			94.45 \pm 0.84

Table 3: Mean plus/minus one standard deviation of the number of constraint violations by SMAC, TPE, GPyOpt and random search within 16 BO iterations over 8 random initializations, for constraint violation penalties of 500, 250 and 125 nats.

Algorithm	Penalty (nats)		
	500	250	125
SMAC	37 \pm 21.7	36 \pm 21.9	28 \pm 11.6
TPE	67 \pm 21.3	68 \pm 22.2	68 \pm 22.2
GPyOpt	36 \pm 19.3	32 \pm 18.0	27 \pm 10.4
Random search	71 \pm 25.5	71 \pm 25.5	71 \pm 25.5

B.4 Visualization of Reconstruction Quality

While log-likelihood scores allow for a principled quantitative comparison between different algorithms, they are typically hard to interpret for humans. We thus in Fig. 5 visualize the reconstruction quality achieved by the best VAE configuration found by the different methods after 32 BO iterations. The VAEs were trained for 32 epochs each (as in the BO experiments). The log-likelihood scores seem to be correlated with quality of visual appearance, and the model found by MiVABO thus may be perceived to produce the visually most appealing reconstructions among all models.

C Pseudo-Code for Thompson Sampling

$$\begin{aligned}
 p(\mathbf{w}|\mathbf{X}_{1:t}, \mathbf{y}_{1:t}) &= \mathcal{N}(\mathbf{m}, \mathbf{S}^{-1}), \quad \text{where} \\
 \mathbf{m} &= \beta \mathbf{S}^{-1} \Phi_{1:t}^\top \mathbf{y}_{1:t} = \beta \mathbf{S}^{-1} (\sum_{\tau=1}^t \phi(\mathbf{x}_\tau) y_\tau), \\
 \mathbf{S} &= \alpha \mathbf{I} + \beta \Phi_{1:t}^\top \Phi_{1:t} = \alpha \mathbf{I} + \beta \sum_{\tau=1}^t \phi(\mathbf{x}_\tau) \phi(\mathbf{x}_\tau)^\top
 \end{aligned}$$

Algorithm 1 THOMPSON SAMPLING

Require: model features $\phi(\mathbf{x})$

- 1: Set $\mathbf{S} = \mathbf{I}$, $\mathbf{m} = \mathbf{0}$
- 2: **for** $t = 1, 2, \dots, T$ **do**
- 3: Sample $\tilde{\mathbf{w}}_t \sim \mathcal{N}(\mathbf{m}, \mathbf{S}^{-1})$
- 4: Select input $\mathbf{x}_t \in \arg \max_{\mathbf{x} \in \mathcal{X}} \tilde{\mathbf{w}}_t^\top \phi(\mathbf{x})$
- 5: Query output $y_t = f(\mathbf{x}_t) + \epsilon$
- 6: Update \mathbf{S}, \mathbf{m} according to Appendix C.
- 7: **end for**
- 8: **Output:** $\tilde{\mathbf{x}}_* \in \arg \max_{\mathbf{x} \in \mathcal{X}} \mathbf{m}^\top \phi(\mathbf{x})$

D Description of Dual Decomposition

A way to maximize acquisition function in Eq. (2) is via dual decomposition - a powerful approach based on Lagrangian optimization, which has well-studied theoretical properties and has been successfully used for many different problems [31, 57, 50]. Despite its versatility, the core idea is simple: decompose the initial problem into smaller solvable subproblems and then extract a solution by cleverly combining the solutions from these subproblems [31]. This requires the following two components: (1) A set of *subproblems* which are defined such that their sum corresponds to the optimization objective, and which can each be optimized globally, and (2) a so-called *master* problem that coordinates the subproblems to find a solution to the original problem. One major advantage of dual decomposition algorithms is that they have well-understood theoretical properties¹³, in particular through connections to linear programming (LP) relaxations. In fact, they enjoy the best theoretical guarantees in terms of convergence properties, when compared to other algorithms solving this problem [31].

We now describe how to devise a dual decomposition for our problem, by demonstrating how it can be reformulated in terms of master- and sub-problems (see Appendix E for a detailed derivation). For convenience, let us denote the discrete, continuous and mixed parts of Eq. (2) by $f^d(\mathbf{x}^d) = \mathbf{w}^d \top \phi^d(\mathbf{x}^d)$, $f^c(\mathbf{x}^c) = \mathbf{w}^c \top \phi^c(\mathbf{x}^c)$ and $f^m(\mathbf{x}^d, \mathbf{x}^c) = \mathbf{w}^m \top \phi^m(\mathbf{x}^d, \mathbf{x}^c)$, respectively, thus resulting in the representation $f(\mathbf{x}) = f^d(\mathbf{x}^d) + f^c(\mathbf{x}^c) + f^m(\mathbf{x}^d, \mathbf{x}^c)$. First, we note that the discrete $f^d(\mathbf{x}^d)$ and continuous $f^c(\mathbf{x}^c)$ parts of Eq. (2) already represent easy to solve subproblems (as we assume to have access to an optimization oracle). It thus remains to discuss the mixed part $f^m(\mathbf{x}^d, \mathbf{x}^c)$. As f^m is generally difficult to optimize directly, we assume that it decomposes into a sum $f^m(\mathbf{x}) = \sum_{k=1}^{|F|} f_k^m(\mathbf{x}_k^d, \mathbf{x}_k^c)$ of so-called *factors* $f_k^m : \mathcal{X}_k^d \times \mathcal{X}_k^c \rightarrow \mathbb{R}$, where $\mathbf{x}_k^d \in \mathcal{X}_k^d$ and $\mathbf{x}_k^c \in \mathcal{X}_k^c$ respectively denote subvectors of \mathbf{x}^d and \mathbf{x}^c from the (typically low-dimensional) subspaces $\mathcal{X}_k^d \subseteq \mathcal{X}^d$ and $\mathcal{X}_k^c \subseteq \mathcal{X}^c$. Here, F denotes a set of subsets $k \in F$ of the variables. Given this formulation, the initial problem then reduces¹⁴ to the minimization of the dual function $L(\boldsymbol{\lambda})$ w.r.t. Lagrange multipliers $\boldsymbol{\lambda}$, i.e., the master problem $\min_{\boldsymbol{\lambda}} L(\boldsymbol{\lambda})$, with dual function $L(\boldsymbol{\lambda}) = \max_{\mathbf{x}^d} \{f^d(\mathbf{x}^d) + \sum_{k \in F} \boldsymbol{\lambda}_k^d \mathbf{x}_{|k}^d\} + \max_{\mathbf{x}^c} \{f^c(\mathbf{x}^c) + \sum_{k \in F} \boldsymbol{\lambda}_k^c \mathbf{x}_{|k}^c\} + \sum_{k \in F} \max_{\mathbf{x}_k^d, \mathbf{x}_k^c} \{f_k^m(\mathbf{x}_k^d, \mathbf{x}_k^c) - \boldsymbol{\lambda}_k^d \mathbf{x}_k^d - \boldsymbol{\lambda}_k^c \mathbf{x}_k^c\}$. Here, the master problem coordinates the $2 + |F|$ maximization subproblems, where $\mathbf{x}_{|k}^d$ and $\mathbf{x}_{|k}^c$ respectively denote the subvectors of \mathbf{x}^d and \mathbf{x}^c containing only the variables of factor $k \in F$, $\boldsymbol{\lambda}_k^d$ and $\boldsymbol{\lambda}_k^c$ are their corresponding Lagrange multipliers. Intuitively, by updating the dual variables $\boldsymbol{\lambda}$, the master problem ensures agreement on the involved variables between the discrete and continuous subproblems and the mixed factors. Importantly, the dual function $L(\boldsymbol{\lambda})$ only involves independent maximization over local assignments of $\mathbf{x}^d, \mathbf{x}^c$ and $\mathbf{x}_k^d, \mathbf{x}_k^c$, which are assumed to be tractable. There are two main classes of algorithms used for the maximization, namely subgradient methods and block coordinate descent [57].

¹³For details, we refer the interested reader to [31, 57, 50]

¹⁴Refer to Appendix E for a detailed derivation.

E Derivation of Dual Decomposition

One interesting interpretation of our acquisition function optimization problem as defined in Section 3.3 is as *maximum a posteriori* (MAP) inference in the undirected graphical model, or Markov random field (MRF) [30], induced by the dependency graph of the involved variables (i.e. the graph in which vertices correspond to variables, and edges appear between variables that interact in some way). We take this perspective and devise a dual decomposition to tackle the MAP estimation problem induced by our particular setting (i.e., interpreting our acquisition function as the energy function of the graphical model), following the formulation of [57].¹⁵

Consider a graphical model on the vertex set $\mathcal{V} = V_d \cup V_c$, where the vertices $V_d = \{1, \dots, D_d\}$ and $V_c = \{D_d + 1, \dots, D_d + D_c\}$ correspond to the discrete and continuous variables $\mathbf{x}^d \in \mathcal{X}^d$ and $\mathbf{x}^c \in \mathcal{X}^c$, respectively. Furthermore, consider a set F of subsets of both discrete and continuous variables/vertices, i.e., $\forall f \in F : f = (f^d \cup f^c) \subseteq \mathcal{V}$, $\emptyset \neq f^d \subseteq V_d$, $\emptyset \neq f^c \subseteq V_c$, where each subset corresponds to the domain of one of the factors.

Now assume that we are given the following functions on these factors as well as on all discrete/continuous variables:

- A factor $\theta^d(\mathbf{x}^d), \theta^d : \mathcal{X}^d \rightarrow \mathbb{R}$ on all discrete variables
- A factor $\theta^c(\mathbf{x}^c), \theta^c : \mathcal{X}^c \rightarrow \mathbb{R}$ on all continuous variables
- $|F|$ mixed factors $\theta_f^m(\mathbf{x}_f^d, \mathbf{x}_f^c), \theta_f^m : \mathcal{X}_f^d \times \mathcal{X}_f^c \rightarrow \mathbb{R}$ on subsets $f \in F$ of both discrete and continuous variables, where $\mathbf{x}_f^d \in \mathcal{X}_f^d$ and $\mathbf{x}_f^c \in \mathcal{X}_f^c$ respectively denote subvectors of \mathbf{x}^d and \mathbf{x}^c from the (typically low-dimensional) subspaces $\mathcal{X}_f^d \subseteq \mathcal{X}^d$ and $\mathcal{X}_f^c \subseteq \mathcal{X}^c$, indexed by the vertices contained in f

The goal of our MAP problem is to find and assignment to all variables \mathbf{x}^d and \mathbf{x}^c which maximizes the sum of the factors:

$$\text{MAP}(\boldsymbol{\theta}) = \max_{\mathbf{x}} \left\{ \theta^d(\mathbf{x}^d) + \theta^c(\mathbf{x}^c) + \sum_{f \in F} \theta_f^m(\mathbf{x}_f^d, \mathbf{x}_f^c) \right\} \quad (9)$$

We now slightly reformulate this problem by duplicating the variables x_i^d and x_j^c , once for each mixed factor $\theta_f^m(\mathbf{x}_f^d, \mathbf{x}_f^c)$, and then enforce that these variables are equal to the ones appearing in the factors $\theta^d(\mathbf{x}^d)$ and $\theta^c(\mathbf{x}^c)$, respectively. Let x_i^{df} and x_j^{cf} respectively denote the copy of x_i^d and x_j^c used by factor f . Moreover, denote by $\mathbf{x}_f^{df} = \{x_i^{df}\}_{i \in f^d}$ and $\mathbf{x}_f^{cf} = \{x_j^{cf}\}_{j \in f^c}$ the set of variables used by factor f , and by $\mathbf{x}^F = \{\mathbf{x}_f^{df}, \mathbf{x}_f^{cf}\}_{f \in F}$ the set of all variable copies. We then get the equivalent (but now constrained) optimization problem

$$\begin{aligned} & \max_{\mathbf{x}, \mathbf{x}^F} \left\{ \theta^d(\mathbf{x}^d) + \theta^c(\mathbf{x}^c) + \sum_{f \in F} \theta_f^m(\mathbf{x}_f^{df}, \mathbf{x}_f^{cf}) \right\} \\ \text{s.t. } & x_i^{df} = x_i^d, \quad \forall f \in F, i \in f^d \\ & x_j^{cf} = x_j^c, \quad \forall f \in F, j \in f^c \end{aligned} \quad (10)$$

To remove the coupling constraints, [57] now propose to use the technique of *Lagrangian relaxation* and introduce a Lagrange multiplier / dual variable $\lambda_{fi}(x_i)$ for every choice of $f \in F$, $i \in f$ and x_i (i.e. for every factor, for every variable in that factor, and for every value of that variable). These multipliers may then be interpreted as the *message* that factor f sends to variable i about its state x_i .

While this works well if all variables are discrete, in our model we however also have continuous variables x_j^c , and it is clearly not possible to have a Lagrange multiplier for every possible value of x_j^c . To mitigate this issue, we follow [31] and instead only introduce a multiplier λ_{fi} for every choice of $f \in F$ and $i \in f$, and model the interaction with the variables as $\lambda_{fi}(x_i) = \lambda_{fix_i}$ (i.e.,

¹⁵In accordance with the notation in [57], we will here denote the factors by θ instead of f (i.e., in contrast to the main text).

the product of a multiplier λ_{fi} and variable x_i). Observe that since our goal is to relax the coupling constraints, it is sufficient to introduce one multiplier per constraint. Since we have a constraint for every factor $f \in F$ and every discrete variable $i \in f^d$ and continuous variable $j \in f^c$ in that factor, our approach is clearly viable.

Note that in contrast to [31], who introduce a set of multipliers for *every* factor / subgraph, we only introduce multipliers for the *mixed* factors $f \in F$. This is because in contrast to [31], we don't introduce a full set of variable copies for *every* factor and then couple them to another global set of "original" variables, but we instead only introduce variable copies for the *mixed* factors and couple them to the variables appearing in the *discrete and continuous* factors, which we assume to be the "original" variables instead. This essentially is the same approach used in [57], with the difference that [57] introduce a singleton factor for each variable (i.e., a factor which depends only on a single variable), which they consider to be the "original" variable. They then simply couple the variable copies appearing in the *higher-order* factors to the "original" variables appearing in the *singleton* factors. In contrast, in our formulation we don't introduce singleton factors to model the "original" variables, but instead use the *fully discrete and continuous* factors for this purpose, which clearly works equally well. Note that as a result of this modeling choice, our optimization problem will be unconstrained, regardless of the number of factors, similar as in [57]. In contrast, [31] end up with constraints enforcing that some of the dual variables sum to zero, since they are optimizing out the global set of "original" variables from their objective, while we keep the set of "original" variables within our discrete and continuous factors. For this reason, we will in contrast to [31] later not require a projection step within the subgradient method used to optimize the dual; this is to be detailed further below.

For clarity, we treat discrete and continuous variables distinctly and for factor $f \in F$ denote λ_{fi}^d and λ_{fj}^c respectively for the Lagrange multipliers corresponding to its discrete variables $i \in f^d$ (or rather, the constraints $x_i^{df} = x_i^d$) and its continuous variables $j \in f^c$ (or rather, the constraints $x_j^{cf} = x_j^c$). For every factor $f \in F$, we furthermore aggregate its multipliers into the vectors $\boldsymbol{\lambda}_f^d = \{\lambda_{fi}^d\}_{i \in f^d} \in \mathbb{R}^{|\mathcal{X}_f^d|}$ and $\boldsymbol{\lambda}_f^c = \{\lambda_{fj}^c\}_{j \in f^c} \in \mathbb{R}^{|\mathcal{X}_f^c|}$. The set of all Lagrange multipliers is thus $\boldsymbol{\lambda} = \{\lambda_{fi}^d : f \in F, i \in f^d\} \cup \{\lambda_{fj}^c : f \in F, j \in f^c\} = \{\boldsymbol{\lambda}_f^d, \boldsymbol{\lambda}_f^c\}_{f \in F}$. We then define the Lagrangian

$$\begin{aligned}
L(\boldsymbol{\lambda}, \mathbf{x}, \mathbf{x}^F) &= \theta^d(\mathbf{x}^d) + \theta^c(\mathbf{x}^c) + \sum_{f \in F} \theta_f^m(\mathbf{x}_f^{df}, \mathbf{x}_f^{cf}) \\
&+ \sum_{f \in F} \sum_{i \in f^d} \lambda_{fi}^d (x_i^d - x_i^{df}) + \sum_{f \in F} \sum_{j \in f^c} \lambda_{fj}^c (x_j^c - x_j^{cf}) \\
&= \left(\theta^d(\mathbf{x}^d) + \sum_{f \in F} \sum_{i \in f^d} \lambda_{fi}^d x_i^d \right) \\
&+ \left(\theta^c(\mathbf{x}^c) + \sum_{f \in F} \sum_{j \in f^c} \lambda_{fj}^c x_j^c \right) \\
&+ \sum_{f \in F} \left(\theta_f^m(\mathbf{x}_f^{df}, \mathbf{x}_f^{cf}) - \sum_{i \in f^d} \lambda_{fi}^d x_i^{df} - \sum_{j \in f^c} \lambda_{fj}^c x_j^{cf} \right).
\end{aligned}$$

This results in the following optimization problem:

$$\begin{aligned}
&\max_{\mathbf{x}, \mathbf{x}^F} L(\boldsymbol{\lambda}, \mathbf{x}, \mathbf{x}^F) \\
\text{s.t. } &x_i^{df} = x_i^d, \quad \forall f \in F, i \in f^d \\
&x_j^{cf} = x_j^c, \quad \forall f \in F, j \in f^c
\end{aligned} \tag{11}$$

Note that the problem in Eq. (11) is still equivalent to our (hard) original problem in Eq. (9) for any assignment of $\boldsymbol{\lambda}$, since the Lagrange multipliers cancel out if all coupling constraints are fulfilled.

To obtain a tractable problem, we thus simply omit the coupling constraints in Eq. (11) and define the dual function $L(\boldsymbol{\lambda})$ as

$$\begin{aligned}
L(\boldsymbol{\lambda}) &= \max_{\mathbf{x}, \mathbf{x}^F} L(\boldsymbol{\lambda}, \mathbf{x}, \mathbf{x}^F) \\
&= \max_{\mathbf{x}^d} \left(\theta^d(\mathbf{x}^d) + \sum_{f \in F} \sum_{i \in f^d} \lambda_{fi}^d x_i^d \right) \\
&\quad + \max_{\mathbf{x}^c} \left(\theta^c(\mathbf{x}^c) + \sum_{f \in F} \sum_{j \in f^c} \lambda_{fj}^c x_j^c \right) \\
&\quad + \sum_{f \in F} \max_{\mathbf{x}_f^{df}, \mathbf{x}_f^{cf}} \left(\theta_f^m(\mathbf{x}_f^{df}, \mathbf{x}_f^{cf}) - \sum_{i \in f^d} \lambda_{fi}^d x_i^{df} - \sum_{j \in f^c} \lambda_{fj}^c x_j^{cf} \right)
\end{aligned}$$

Note that the maximizations are now fully independent, such that we can (without introducing any ambiguity) simplify the notation for the variables involved in the mixed terms to denote \mathbf{x}_f^d and \mathbf{x}_f^c instead of \mathbf{x}_f^{df} and \mathbf{x}_f^{cf} , respectively¹⁶, resulting in the slightly simpler dual formulation

$$\begin{aligned}
L(\boldsymbol{\lambda}) &= \max_{\mathbf{x}^d} \left(\theta^d(\mathbf{x}^d) + \sum_{f \in F} \sum_{i \in f^d} \lambda_{fi}^d x_i^d \right) \\
&\quad + \max_{\mathbf{x}^c} \left(\theta^c(\mathbf{x}^c) + \sum_{f \in F} \sum_{j \in f^c} \lambda_{fj}^c x_j^c \right) \\
&\quad + \sum_{f \in F} \max_{\mathbf{x}_f^d, \mathbf{x}_f^c} \left(\theta_f^m(\mathbf{x}_f^d, \mathbf{x}_f^c) - \sum_{i \in f^d} \lambda_{fi}^d x_i^d - \sum_{j \in f^c} \lambda_{fj}^c x_j^c \right)
\end{aligned}$$

Let $\mathbf{x}_{|f}^d \in \mathcal{X}_f^d$ and $\mathbf{x}_{|f}^c \in \mathcal{X}_f^c$ respectively denote the subvectors of \mathbf{x}^d and \mathbf{x}^c containing only the variables of factor f . The shorthands (or *reparameterizations* [57])

$$\begin{aligned}
\bar{\theta}_d^{\boldsymbol{\lambda}}(\mathbf{x}^d) &= \theta^d(\mathbf{x}^d) + \sum_{f \in F} \sum_{i \in f^d} \lambda_{fi}^d x_i^d \\
&= \theta^d(\mathbf{x}^d) + \sum_{f \in F} \boldsymbol{\lambda}_f^d \mathbf{x}_{|f}^d
\end{aligned} \tag{12}$$

$$\begin{aligned}
\bar{\theta}_c^{\boldsymbol{\lambda}}(\mathbf{x}^c) &= \theta^c(\mathbf{x}^c) + \sum_{f \in F} \sum_{j \in f^c} \lambda_{fj}^c x_j^c \\
&= \theta^c(\mathbf{x}^c) + \sum_{f \in F} \boldsymbol{\lambda}_f^c \mathbf{x}_{|f}^c
\end{aligned} \tag{13}$$

$$\begin{aligned}
\bar{\theta}_f^{\boldsymbol{\lambda}}(\mathbf{x}_f^d, \mathbf{x}_f^c) &= \theta_f^m(\mathbf{x}_f^d, \mathbf{x}_f^c) - \sum_{i \in f^d} \lambda_{fi}^d x_i^d - \sum_{j \in f^c} \lambda_{fj}^c x_j^c \\
&= \theta_f^m(\mathbf{x}_f^d, \mathbf{x}_f^c) - \boldsymbol{\lambda}_f^d \mathbf{x}_f^d - \boldsymbol{\lambda}_f^c \mathbf{x}_f^c
\end{aligned} \tag{14}$$

further simplify the dual function $L(\boldsymbol{\lambda})$ to

$$L(\boldsymbol{\lambda}) = \max_{\mathbf{x}^d} \bar{\theta}_d^{\boldsymbol{\lambda}}(\mathbf{x}^d) + \max_{\mathbf{x}^c} \bar{\theta}_c^{\boldsymbol{\lambda}}(\mathbf{x}^c) + \sum_{f \in F} \max_{\mathbf{x}_f^d, \mathbf{x}_f^c} \bar{\theta}_f^{\boldsymbol{\lambda}}(\mathbf{x}_f^d, \mathbf{x}_f^c). \tag{15}$$

First, observe that since we maximize over \mathbf{x} and \mathbf{x}^F , the dual function $L(\boldsymbol{\lambda})$ is a function of just the Lagrange multipliers $\boldsymbol{\lambda}$. Note that since $L(\boldsymbol{\lambda})$ maximizes over a larger space (since instead of forcing that there must be one global assignment maximizing the objective, we allow the discrete/continuous

¹⁶I.e., we replace all variable copies $\mathbf{x}_f^{df}, \mathbf{x}_f^{cf}$ in the mixed terms by the "original" variables $\mathbf{x}_f^d, \mathbf{x}_f^c$.

potentials to be maximized independently of the mixed potentials, meaning that \mathbf{x} may not coincide with \mathbf{x}^F), we have for all $\boldsymbol{\lambda}$ that

$$\text{MAP}(\boldsymbol{\theta}) \leq L(\boldsymbol{\lambda}) . \quad (16)$$

The *dual problem* now is to find the tightest upper bound by optimizing the Lagrange multipliers, i.e.

$$\min_{\boldsymbol{\lambda}} L(\boldsymbol{\lambda}) \quad (17)$$

We also call the dual problem in Eq. (17) the *master problem*, which coordinates the $2 + |F|$ *slave problems* (i.e., one for each factor)

$$s^d(\boldsymbol{\lambda}) = \max_{\mathbf{x}^d} \bar{\theta}_d^{\boldsymbol{\lambda}}(\mathbf{x}^d) \quad (18a)$$

$$s^c(\boldsymbol{\lambda}) = \max_{\mathbf{x}^c} \bar{\theta}_c^{\boldsymbol{\lambda}}(\mathbf{x}^c) \quad (18b)$$

$$s^f(\boldsymbol{\lambda}) = \max_{\mathbf{x}_f^d, \mathbf{x}_f^c} \bar{\theta}_f^{\boldsymbol{\lambda}}(\mathbf{x}_f^d, \mathbf{x}_f^c), \quad \forall f \in F . \quad (18c)$$

where we refer to s^d , s^c and s^f as the discrete slave, the continuous slave, and the mixed slaves, respectively. Using the notation in Eqs. (18a)-(18c), the dual function further simplifies to

$$L(\boldsymbol{\lambda}) = s^d(\boldsymbol{\lambda}) + s^c(\boldsymbol{\lambda}) + \sum_{f \in F} s^f(\boldsymbol{\lambda}) . \quad (19)$$

Intuitively, the goal of Eq. (17) is as follows: The master problem wants the discrete/continuous slaves to agree with the mixed slaves/factors in which the corresponding discrete/continuous variables appear, and conversely, it wants the mixed slaves to agree with the slaves/factors of the discrete/continuous variables in its scope. The master problem will thus incentivize the discrete/continuous slaves and the mixed slaves to agree with each other, which is done by updating the dual variables $\boldsymbol{\lambda}$ accordingly.

The key property of the function $L(\boldsymbol{\lambda})$ is that it only involves maximization over local assignments of \mathbf{x}^d , \mathbf{x}^c and $\mathbf{x}_f^d, \mathbf{x}_f^c$, which are tasks we assume to be tractable. The dual thus decouples the original problem, resulting in a problem that can be optimized using local operations. Algorithms that minimize the approximate objective $L(\boldsymbol{\lambda})$ use local updates where each iteration of the algorithms repeatedly finds a maximizing assignment for the subproblems individually, using these to update the dual variables $\boldsymbol{\lambda}$ that glue the subproblems together. There are two main classes of algorithms of this kind, one based on a subgradient method and another based on block coordinate descent [57].

F Details on Baseline Implementations and XGBoost Benchmark

We use the publicly available Python implementations of SMAC [25] (<https://github.com/automl/SMAC3>), TPE [7] (<https://github.com/hyperopt/hyperopt>), and GPyOpt [17] (<https://github.com/SheffieldML/GPyOpt>).

Furthermore, please refer to the corresponding websites for details on the OpenML XGBoost benchmark (<https://www.openml.org/f/6767>), on the underlying implementation (<https://www.rdocumentation.org/packages/xgboost/versions/0.6-4>), and on the steel-plates-fault (<https://www.openml.org/t/9967>) and monks-problem-1 (<https://www.openml.org/t/146064>) datasets.

Finally, see Table 4 for a description of the hyperparameters involved in XGBoost.

Table 4: Hyperparameters of the XGBoost algorithm. 10 parameters, 3 of which are discrete.

Name	Type	Domain
booster	discrete	[‘gbtree’, ‘gblinear’]
nrounds	discrete	[3, 5000]
alpha	continuous	[0.000985, 1009.209690]
lambda	continuous	[0.000978, 999.020893]
colsample_bylevel	continuous	[0.046776, 0.998424]
colsample_bytree	continuous	[0.062528, 0.999640]
eta	continuous	[0.000979, 0.995686]
max_depth	discrete	[1, 15]
min_child_weight	continuous	[1.012169, 127.041806]
subsample	continuous	[0.100215, 0.999830]

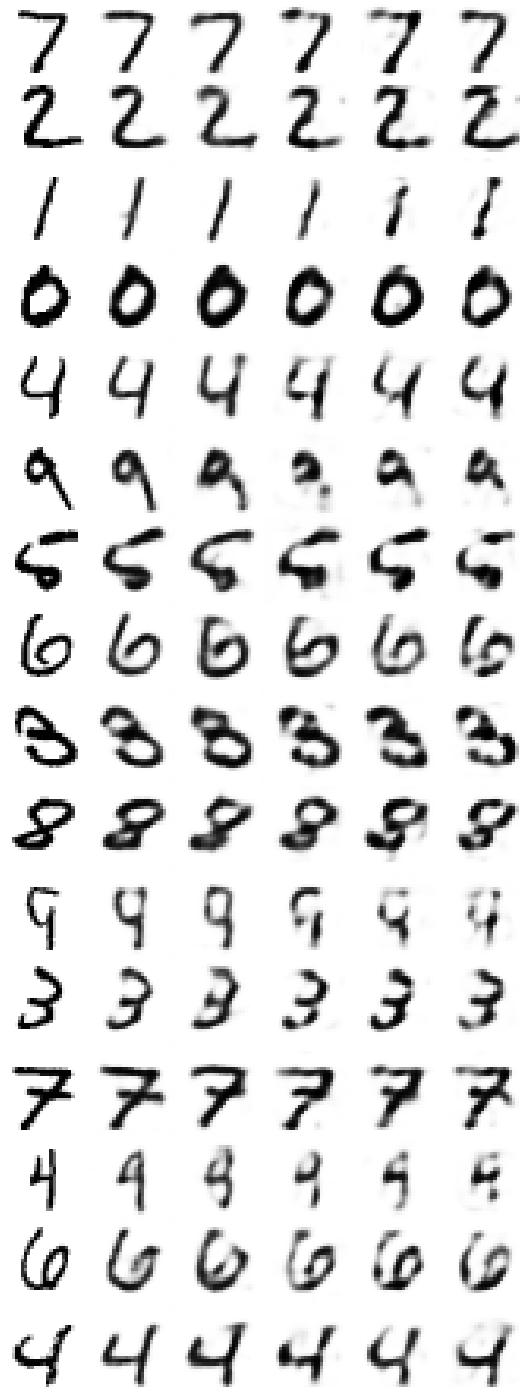


Figure 5: Visualization of the reconstruction quality of a random subset of (non-binarized) images from the MNIST test set, as achieved by the best VAE model (trained for 32 epochs) found by each method. From left to right: ground truth, MIVABO, random search, GPyOpt, TPE and SMAC. The images are thus ordered (from left to right) by increasing negative test log-likelihood achieved by the VAEs used for reconstruction. Interestingly, the log-likelihood seems to capture quality of visual appearance, as the reconstruction quality may be roughly perceived to decrease from left to right.